Theory and computational modeling of the 30 nm chromatin fiber

Jörg Langowski[1] and Helmut Schiessel[2]

[1] Division Biophysics of Macromolecules (B040), Deutsches Krebsforschungszentrum, Im Neuenheimer Feld 580, D-69120 Heidelberg, Germany; e-mail: jl@dkfz.de

[2] Max Planck Institute for Polymer Research, Theory group, PO Box 3148, D-55021 Mainz; Germany, e-mail: heli@mpip-mainz.mpg.de

Introduction

For its fundamental importance in gene regulation and epigenetics, the physical chemistry of structural changes in the chromatin fiber has become a major focus of interest in recent years. It is now clear that the mechanism of chromatin remodeling, opening and closing of the structure during transcription, and many other biological processes related to the higher order structure of the genome cannot be understood without fundamental knowledge of the arrangement of nucleosomes and DNA in the chromatin fiber and its variations during different physiological states of the cell.

The 'bead-chain' structure of nucleosomes spaced regularly on DNA will compact into a higher order structure under physiological conditions. The generally accepted view is that the first stage of compaction of the nucleosome chain is a fiber-like structure with a diameter of approximately 30 nm, the so-called '30-nm fiber', although alternative structures have been proposed (e.g. the 'superbeads' seen in electron microscopy images by Zentgraf and Franke [1]). Since the discovery of the bead-chain structure of chromatin by Olins and Olins[2; 3] and Woodcock[4], many attempts have been made to construct models for the path of the DNA inside this fiber and its possible conformations. Although many new insights have been obtained, the picture is not yet conclusive and the precise arrangement of DNA and histones inside the 30 nm fiber is still controversial [5; 6; 7; 8]. Mainly two competing classes of models have been discussed: the *solenoid* models [9; 10; 11]; and the *zig-zag* or *crossed-linker* models [12; 13; 14; 15; 16; 17]. In the solenoid model (Fig. 1a) it is assumed that the chain of nucleosomes forms a helical structure with the nucleosome axis being almost perpendicular

to the solenoid axis. The DNA entry-exit side faces inward towards the axis of the solenoid. The linker DNA is required to be bent in order to connect neighboring nucleosomes in the solenoid. The other class of models assumes *straight* linkers that connect nucleosomes located on opposite sides of the fiber. The axis of the nucleosomal disk is only slightly tilted with respect to the fiber direction. The resulting linker geometry shows a three-dimensional zig-zag-like pattern (Fig. 1b).

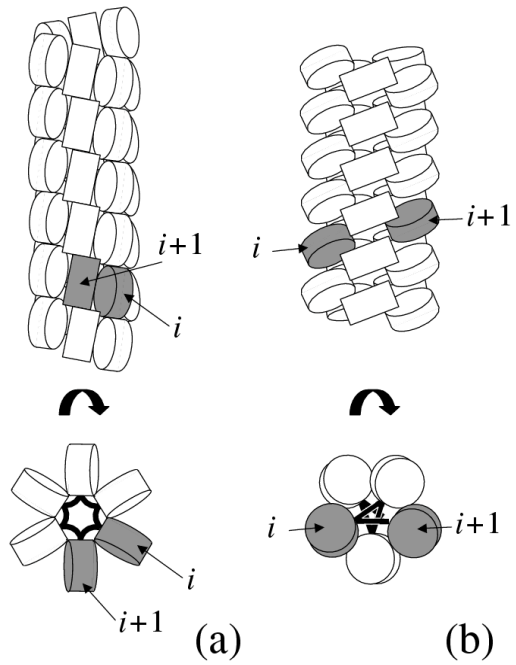

Fig. 1: The two competing classes of models for the 30-nm fiber can be distributed into (a) solenoid models and (b) crossed-linker models. For both fiber types the side and the top view are shown. Two nucleosomes that are directly connected via DNA linker are shaded in grey. In the solenoid these nucleosomes are located on the same side of the fiber requiring the linker to be bent. In the crossed-linker case they sit on opposite sides of the fiber and are connected via a straight linker.

Images obtained by cryo electron microscopy should in principle be able to distinguish between the structural features proposed by the different models mentioned above [16]. The micrographs show a zig-zag motif at lower salt concentrations and they indicate that the chromatin fiber becomes more and more compact when the ionic strength is raised towards the physiological value (i.e. about 150 mM monovalent ions).

From the physics point of view, the system that we deal with here – a semiflexible polyelectrolyte that is packaged by protein complexes regularly spaced along its contour – is of a complexity that

still allows the application of analytical and numerical models. For quantitative prediction of chromatin properties from such models, certain physical parameters must be known such as the dimensions of the nucleosomes and DNA, their surface charge, interactions, and mechanical flexibility. Current structural research on chromatin, oligonucleosomes and DNA has brought us into a position where many such elementary physical parameters are known. Thus, our understanding of the components of the chromatin fiber is now at a level where predictions of physical properties of the fiber are possible and can be experimentally tested.

Computational modeling can be a very powerful tool to understand the structure and dynamics of complex supramolecular assemblies in biological systems. We need to sharpen the definition of the term 'model' somewhat, designating a procedure that allows us to *quantitatively* predict the physical properties of the system. In that sense, the simple geometrical illustrations in Fig. 1 only qualify if by some means experimentally accessible parameters can be calculated. As an example, a quantitative treatment of DNA bending in the solenoid model would only be possible if beyond the mechanical and charge properties of DNA and nucleosomes the energetics of linker DNA-histone and nucleosome-nucleosome interaction necessary to overcome the elastic stress in the DNA due to the bend were quantitatively known. The straight linker configuration offers the advantage for modeling that the geometry and the energetics of the fiber are controlled to a large extent by the linker DNA, whose conformations and mechanical properties are very well understood, and its energetics are favorable because no energy is required to bend the DNA. It therefore comes as no surprise that most recent numerical and analytical models assume straight linkers (at elastic equilibrium, notwithstanding thermal fluctuations, v.i.), which is also supported by current experimental data.

In this chapter we attempt to give an overview of current computational modeling approaches of the 30 nm fiber, their capabilities and limitations. In order to setup a quantitative model of this supramolecular assembly, we first need to understand the physical properties of its subcomponents: nucleosomes and DNA.

Physical properties of nucleosomes and DNA

DNA, on a length scale beyond some tens of base pairs, can be described as a stiff polymer chain with an electrostatic charge. In the most basic view, four parameters are sufficient to describe this chain with sufficient precision: the diameter, the elastic constants for bending and torsion and the electrostatic potential.

The average DNA helix diameter used in modeling applications such as the ones described here includes the diameter of the atomic-scale B-DNA structure and – approximately – the thickness of the hydration shell and ion layer closest to the double helix [18]. Both for the calculation of the electrostatic potential and the hydrodynamic properties of DNA (i.e. the friction coefficient of the helix for viscous drag) a helix diameter of 2.4 nm describes the chain best [19; 20; 21; 22]. The choice of this parameter was supported by the results of chain knotting [23] or catenation [24], as well as light scattering [25] and neutron scattering [26] experiments.

The bending elasticity of the DNA chain can be expressed as the *bending persistence length* L_p, the distance over which the average cosine of the angle between the two chain ends has decayed to 1/e. Molecules shorter than L_p behave approximately like a rigid rod, while longer chains show significant internal flexibility. The bending elasticity A - the energy required to bend a polymer segment of unit length over an angle of 1 radian - is related to the persistence length by $L_p = A/k_BT$, k_B being Boltzmann's constant and T the absolute temperature. For DNA, L_p has been determined in a number of experiments (for a recent compilation, see [27]). While some uncertainties remain as regards the value at very high or low salt concentrations, the existing data agree on a consensus value of L_p = 45-50 nm (132-147 bp) at intermediate ionic strengths (10-100 mM NaCl and/or 0.1-10 μM Mg^{2+}).

The torsional elasticity C, defined as the energy required to twist a polymer segment of unit length through an angle of 1 radian, may be related in an analogous way to a *torsional persistence length* L_T, which is the correlation length of the torsional orientation of a vector normal to the chain axis. Again, C is related to L_T by $L_T = C/k_BT$. C has been measured by various techniques, including

fluorescence polarization anisotropy decay [28; 29; 30] and DNA cyclization [31; 32; 33], and the published values converge on a torsional persistence length of 65 nm (191 bp).

The stretching elasticity of DNA has been measured by single molecule experiments[34; 35] and also calculated by molecular dynamics simulations[36; 37]. One may estimate the stretching elasticity of DNA to be given by a stretching modulus γ of about 1500 pN, where $\sigma = F \cdot \Delta L / L_0$ (ΔL being the extension of a chain of length L_0 by the force F). We may safely assume that DNA stretching does not play a significant role in chromatin structural transitions, since much smaller forces are already causing large distortions of the 30 nm fiber (see below).

The structure of the second important component of the chromatin fiber, the histone octamer[38] resp. the nucleosome[39], has been determined by X-ray crystallography to atomic resolution. From this structure, one can approximate the overall dimensions of the nucleosome as a flat disk of 11 nm diameter and 5.5 nm thickness. The mechanical properties of the nucleosome are not known, and current models take it as nondeformable, which is probably a good approximation in the range of forces usually employed in single-molecule experiments on chromatin fibers (Sivolob et al. showed quite a high stability of nucleosomes even when the DNA was under considerable superhelical stress[40], however the $(H3\text{-}H4)_2$ tetramer showed a structural transition[41]). Also, the nucleosomal DNA is usually assumed as being rigidly attached to the histone core while the elasticity of the DNA at the point where the linker leaves the nucleosome is the same as that for free DNA; the unwrapping of the DNA from the histone core under tension, which is experimentally proven [42; 43], is not yet included in current models, mainly because of lack of quantitative thermodynamic data on core particle-DNA binding. Only very recently a theory has been developed that accounts for tension-induced nucleosome unwrapping; the theoretical predictions of typical unwrapping forces are in good agreement with the experimental observations (I. Kulic and H. Schiessel, preprint cond-mat/0302188).

The interaction between nucleosomes plays an important role for the stability of the 30 nm fiber; recent experiments on liquid crystals of mononucleosomes [44; 45; 46; 47] and also less concentrated mononucleosome solutions [48; 49] show an attractive interaction that can be parameterized by an anisotropic Lennard-Jones type potential [50]. Also, an electrostatic interaction potential has been computed using the crystallographic structure of the nucleosome [51]. The influence of these potentials on the structure of the fiber is discussed below together with the corresponding models.

Computational implementation

The computational description of a large biomolecular complex such as the chromatin fiber requires techniques that are different from the widely applied molecular dynamics methods used to simulate biopolymers at atomic resolution. The current limits (beginning of 2003), for which one can still solve Newton's equations of motion explicitly for each atom in its force fields in a reasonable amount of computer time, are a system size of 10^5 – 10^6 atoms (including the water) and simulation lengths of some nanoseconds. Chromatin fragments of biologically interesting size (i.e., more than 12 nucleosomes) are much more complex, and the times at which typical processes such as nucleosome opening, DNA slipping, etc. take place, are much longer. It is evident that in such a case the biological macromolecule must be described by some approximation.

Energetics: Coarse-graining and interaction potentials

All such approximations are based on 'coarse-graining': subunits are defined that contain many atoms, but behave like rigid objects on the time and length scales considered. As an example, let us look at a chain of 'naked' DNA. If molecular detail is not required, DNA may be approximated by a chain of segments that are substantially shorter than its bending or torsional persistence length; segments up to 50 bp constitute a safe choice. The segments or other subunits interact through appropriate force fields, which can in principle be derived from the interatomic potentials. With the development of all-atom molecular dynamics (MD) in recent years, detailed studies have been possible on the molecular basis of DNA flexibility and on its sequence dependence. While a comprehensive overview of that work falls outside the scope of this article, we would like to

mention some recent studies that can serve as starting points to the reader looking for information in this field: normal-mode analyses of the sequence dependence of DNA flexibility [52; 53] or work from our own laboratory in which DNA flexibility constants are extracted from molecular dynamics trajectories of DNA oligonucleotides[36; 37]. A review of this field is given in [54]. Since the absolute reliability of force constants determined from MD simulations is still limited, however, one usually employs parameters that are determined separately by experiment.

For coarse-grained models of linear biopolymers – such as DNA or chromatin – two types of interactions play a role. The connectivity of the chain implies stretching, bending and torsional potentials, which exist only between directly adjacent subunits and are harmonic for small deviations from equilibrium. As mentioned above, these potentials can be directly derived from the experimentally known persistence length or by directly measuring bulk elastic properties of the chain.

The second type of interactions necessary for modeling the chromatin fiber occurs between non-adjacent subunits of the chain, i.e., contact or other long-range interactions between nucleosomes and/or DNA segments. DNA-DNA interactions in a typical biological environment are mainly due to electrostatic repulsion between the negatively charged backbone phosphates. For intermediate ionic strengths (1 mM – 1 M) and distances larger than about the DNA double helix diameter of 2 nm, these interactions are rather well characterized. A number of simulations simply used an effective hard-core radius, below which the DNA segments are not allowed to approach each other, and which decreases with increasing ionic strength[23; 55; 56; 57; 58; 59]. Other work described the electrostatic interaction through a screened Coulomb potential in the Debye-Hückel approximation, using a renormalized surface charge density for the DNA in order to account for ion condensation[18]. This has the advantage that the dependence of the interaction on the ionic strength does not have to be calibrated empirically, but is contained implicitly in the form of the potential. DNA models based on such potentials have been developed and applied widely in the last two decades, and their predictive power for average solution structural properties, intramolecular interaction kinetics and

other globally measurable parameters is usually very good [19; 20; 21; 22; 26; 60; 61; 62; 63; 64]. One can assume that the approximation of a DNA chain as an elastic filament with Debye-Hückel electrostatics constitutes a safe choice for obtaining a realistic picture of the solution structure.

Less is known about the interaction of the nucleosomes between themselves or with free DNA. The nucleosome-nucleosome interaction has recently been parameterized by using the surface charge density of the known crystal structure [39] in a point-charge model [51]. While in that work only electrostatic interactions were considered and the quantitative influence of the histone tails on the interaction potential still remains obscure, simulations based on this potential allowed to predict an ionic-strength dependent structural transition of a 50-nucleosome chromatin fragment that occurred at a salt concentration compatible with known experimental data (ref.[65], see below).

Nucleosome-nucleosome interaction potentials can be calibrated by comparison with the characteristics of liquid crystals of mononucleosomes at high concentrations. Under suitable conditions, nucleosome core particles form a hexagonal-columnar phase with a distance of 11.55±1□m between the columns and a mean distance of 7.16±0.65□m between the particles in one column[44; 46]. These distances may be assumed to correspond to the positions of the minima of an attractive internucleosomal potential. The depth of the interaction potential (i.e. the binding energy per nucleosome) was estimated in the stretching experiments of Cui and Bustamante[66] to 2.6-3.4 kT. A slightly lower potential minimum of 1.25 kT is obtained by a comparison of the stability of the nucleosome liquid crystal phase with simulations[50].

The DNA-nucleosome interaction parameters are not known at present. In most of the theoretical work it is deemed negligible compared to the DNA-DNA and nucleosome-nucleosome interaction, except for a hard-core excluded volume interaction. Nevertheless, recent work on the mechanism of nucleosome repositioning[67] assumes that the DNA can dynamically detach from the nucleosome surface and reattach in different conformations, such that it is conceivable that distant DNA

segments may also transiently bind to 'open regions' of the DNA-binding surface of the nucleosome.

Mechanics of the chromatin fiber

The conformations of the 'zig-zag' model first proposed by Woodcock et al. [12] and van Holde and Zlatanova [5] are determined by the linker DNA length, the nucleosome shape and two angles: the opening angle α of the linker DNAs at the nucleosome and the twisting angle β between successive nucleosomes on the chain. Since for a given nucleosome spacing (and therefore linker length) the geometry of the resulting chain is uniquely determined by α and β, this model is also called the 'two-angle' model of the chromatin chain. Simply generating conformations of polynucleosome chains with varying values of α and β will create chains that are already very similar to typical conformations of chromatin fibers as seen in cryo-electron microscopy [12] or scanning force microscopy [15].

For the solenoid conformation, few attempts at a quantitative description exist. One notable exception is the work recently presented by Bishop and Hearst[68] and Bishop and Zhmudsky[69]. In their approach the chromatin fiber is described as a continuous 'coiled-coil' filament of an elastic polymer, in which the DNA forms a continuous 11nm diameter spiral that is wound into a 30nm superhelix. The nucleosomes are not assigned to fixed positions, but viewed as bound in a delocalized manner, leading – on average – to a 'fluid-like' structure for the 30 nm fiber. Under these conditions, the chromatin elasticity mostly depends on the mechanical properties of the DNA coil, and the histones may be regarded as some viscous fluid that sticks non-specifically to the DNA surface. This view is rationalized because in its biological function the energy landscape of nucleosome positioning is 'fairly smooth with multiple local minima', because of the rather low specificity of nucleosome positioning. The authors calculate the elastic constants for stretching, shearing and torsion, the linear mass density and moments of inertia for linear DNA and the DNA/histone coil at various degrees of compaction. While qualitative conclusions could be drawn about the relative elasticities of DNA and the chromatin coil, the absolute values of the elasticity

parameters differ quite strongly from the known experimental data in that model. However, with more knowledge about the histone-DNA interaction, the approach by Bishop and coworkers could be valuable for comparing the energetics of zig-zag and solenoid conformations.

For the moment, however, we concentrate here on variants of the two-angle model. We will first give a systematic account on the possible fiber geometries based on straight linkers, then show how the mechanical properties of the model can be understood as being a result of the fiber geometry. It will become clear why it is indispensible to go beyond purely theoretical descriptions, which focus mainly on the geometry and energetics of the linker DNA, to numerical computer models in order to obtain the full picture. It turns out that in determining the fiber properties the interplay between linker DNA stiffness and nucleosome-nucleosome interaction is crucial.

The 'two angle' model – basic notions

Since the linker DNA is assumed straight and the nucleosome non-deformable, the fiber geometry of the two-angle model is completely determined by the entry-exit angle of the linker DNA at each nucleosome and by the rotational angle between neighboring nucleosomes. Depending on the values of these angles and their variation, the structures obtained are either completely regular or more random fibers that resembled real fibers at lower ionic strength. As far as the linker geometry can be detected via cryo-electron microscopy [16] or scanning force microscopy [15; 70], this model indeed describes the geometry of the 30-nm fiber adequately.

Schiessel, Gelbart and Bruinsma [17] introduced a mathematical description for the different possible folding pathways in the two-angle model. At the simplest level, it was assumed that the geometric structure of the 30-nm fiber can be obtained from the intrinsic, single-nucleosome structure where the incoming and outgoing linker chains make an angle α with respect to each other. In the presence of the histone H1 (or H5) the in- and outcoming linker are in close contact forming a stem before they diverge[16].

Next, there is a rotational (dihedral) angle ϕ between the axis of neighboring histone octamers along the necklace (see Fig. 2). Because nucleosomes are rotationally positioned along the DNA, the angle ϕ is a periodic function of the linker length B, with the 10 bp repeat length of the helical twist of DNA as the period. There is experimental evidence that the linker length is preferentially quantized by integral multiples of this helical twist [71], i.e., there is a preferred value of ϕ.

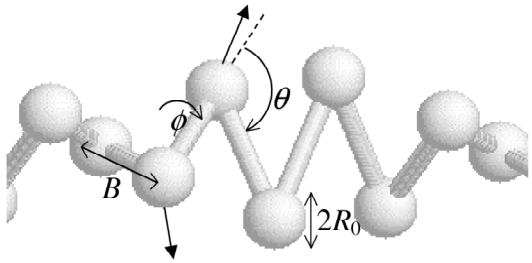

Fig. 2: The geometry of the two-angle fiber can be characterized by the deflection angle θ and the dihedral angle ϕ. Also indicated is B, characterizing the linker length, and the nucleosome diameter $2R_0$. For simplicity, the nucleosomes are represented by spheres connected via links, the linker DNA. The arrows indicate the nucleosomal superhelix axis.

The geometrical structure of the chain in Fig. 2 is determined entirely by q, ϕ and B. The model only describes the linker geometry and does not account for excluded volume effects and other forms of nucleosome-nucleosome interaction; it assumes that the core particles are point-like and that they are located at the joints of the linkers, which are straight rods.

An overview of the possible two-angle fibers is provided in Fig. 3, where q and ϕ are varied over the range 0° to 180° (for a more thorough discussion of the possible structures, see Schiessel and others [17].

Various examples of two-angle fibers were already displayed by Woodcock et al. [12] in their Fig. 2, namely fibers with θ = 150° and many different values of ϕ, corresponding to a vertical trajectory on the right-hand side of Fig. 3. Three different configurations with a fixed value of ϕ and different values of θ are displayed in Fig. 3c in another paper by these authors [16]. Schiessel et al. [17] were able to obtain analytical expressions for all the geometrical quantities that characterize the resulting fiber

as a function of θ, ϕ and B (cf. also [72]). Such quantities are, for instance, the diameter of the fiber, the nucleosome line density or the nucleosomal tilt angle.

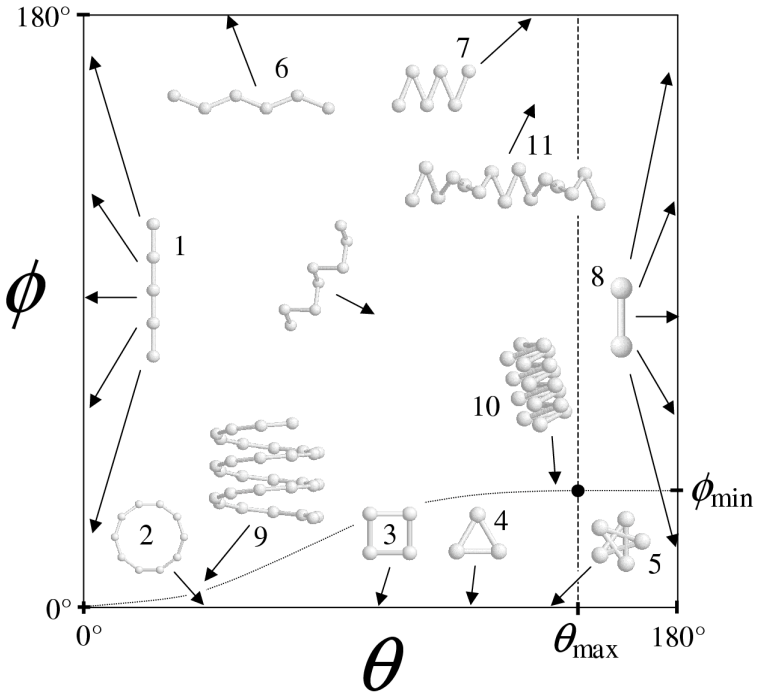

Fig. 3: The full range of the two-angle structures. Shown are some example configurations with the arrows indicating their position in the (θ, ϕ)-plane. The lines denote the boundaries to the forbidden structures where the "nucleosomes" would overlap. To the right of the dashed line nucleosomes *i* and *i*+2 would overlap ("short-range excluded volume"). Below the dotted line nucleosomes further apart with respect to their chemical distance would overlap ("long range excluded volume"). For instance, for the circle, structure "2", nucleosomes collide after one turn (10 nucleosomes).

If one takes into account the excluded volume of the core particles, then certain areas in that phase diagram, Fig. 3, are forbidden – reminiscent of the familiar Ramachandran plots used in the study of protein folding. This is indicated in Fig. 3 by dashed and dotted lines. Except for these regions, however, the diagram in Fig. 3 by itself does not favor any structure over another, since the energetics are not included. Schiessel et al. [17] suggested that the optimum structure for the 30-nm fiber might be a balance between (*i*) *maximum compaction* and (*ii*) *maximum accessibility*, in order to fit the DNA chain into the limited nuclear volume (cf. Ref. [73] to see how severe this packing problem actually is) and to keep local accessibility, which is required for transcription.

In order to attain maximum compaction one needs structures that lead to high bulk densities. A comparison of the densities of all possible structures shows that fibers with internal linkers have highest densities [17]. As detailed there, the highest density is achieved for the largest possible value of α and the smallest possible value of β that is still in accordance with the excluded volume condition, corresponding to the black dot in Fig. 3 where the dotted curve and the dashed line cross each other. This unique set of angles is given by $\alpha_{\max} = 2\arccos(R_0/B)$ and $\beta_{\min} = (8/\alpha)(R_0/B)$. It was suggested in Ref. [17] that maximum accessibility is achieved for structures that, for a given entry-exit angle $\alpha + \beta$ of a highly compacted structure, lead to the maximum reduction in nucleosome line density for a given small change of the angle α. Interestingly, that the such defined accessibility is maximized at the same unique pair of angles ($\alpha_{\max}$, $\beta_{\min}$). The corresponding fiber shows a crossed-linker geometry as depicted in Fig. 1b (cf. also structure "10" in Fig. 3). For reasonable values of the linker length it was found[17] that $\alpha_{\max} = 151°$, $\beta_{\min} = 36°$ together with a nucleosome line density $\rho = 6.9$ nucleosomes per 11 *nm* [72] and a diameter of the order of 30*nm*, values that are close to the experimental ones reported by Bednar et al. [16] for chicken erythrocyte chromatin fibers.

The local accessibility can be controlled *in vitro* by changing the salt concentration. Bednar et al.[16] report, for example, that α decreases with decreasing ionic strength, namely $\alpha = 145°$ at 80 mM, $\alpha = 135°$ at 15 mM and $\alpha = 95°$ at 5 mM [16]. In the biochemical context the change of α can be accomplished by other mechanisms, especially by the depletion of linker histones and the acetylation of core histone tails (cf., for instance [74]), both of which occur in transcriptionally active regions of chromatin (for details compare[75]). . These mechanisms lead effectively to a decrease of α causing the linear nucleosome density to decrease $\rho = 6.0$ (80 mM salt) via $\rho = 3.2$ (15 mM) to $\rho = 1.5$ (5 mM) [16], in good agreement with theoretical predictions[17].

Beyond pure geometry, the two-angle model is also useful to predict some of the *physical properties* of the 30-nm fiber, for instance, its response to elastic stress[17]. In an independent study

on the two-angle model by Ben-Haïm, Lesne and Victor [76] this question has been the major focus, and as demonstrated by Schiessel[72], the elastic properties of the two-angle model as a function of □ and □ are analytically solved completely by combining the results from both papers.

The elastic stress may be external or internal. External stresses are exerted on the chromatin during the cell cycle when the mitotic spindle separates chromosome pairs. The 30-nm fiber should be both highly flexible and extensible to survive these stresses. The *in vitro* experiments by Cui and Bustamante demonstrated that the 30-nm fiber is indeed very "soft" [66]. The 30-nm fiber is also exposed to internal stresses. Attractive or repulsive forces between the nucleosomes will deform the linkers connecting the nucleosomes. For instance, electrostatic interactions, either repulsive (due to the net charge of the nucleosome core particles) or attractive (bridging via the lysine-rich core histone tails[49]) could lead to considerable structural rearrangements.

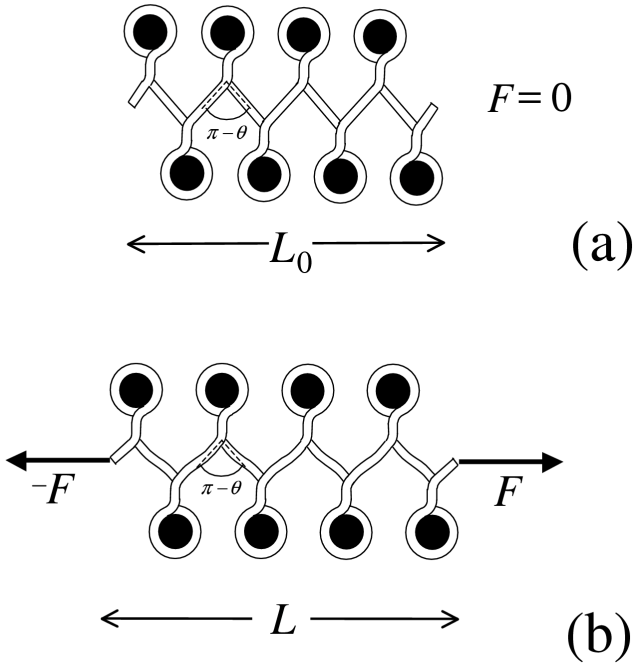

Fig. 4: Two-angle fibers can be easily deformed via the bending and twisting of their linkers. This can be most easily seen for the special case of a planar zig-zag fiber under an external tension F, which extends the fiber via the bending of its linkers from its unperturbed state with contour length L_0 (a) to a stretched state of length $L>L_0$ (b).

It is not the purpose of this chapter to present further mathematical details of the two-angle fiber. We merely mention that its mechanical properties can be described by four moduli, namely the stretching, bending and twisting moduli as well as a twist-stretch coupling constant[76]. Thus the two-angle fiber behaves as an *extensible* worm-like chain as compared to naked DNA that is inextensible for moderate forces. The extensibility of two-angle fibers can be easily understood as a result of the DNA bending/twisting. A special case is depicted in Fig. 4: the planar zig-zag fiber. The external tension F induces an increase of the contour length from the unperturbed value L_0 (Fig. 4 a) to the new value $L > L_0$ (Fig. 4 b). In the zig-zag case this is accomplished via the bending of the linker DNA only. For more general geometries fiber stretching involves linker twisting as well.

The linker backbone is predicted to be very soft: For instance, the stretching modulus of fibers with crossed linkers and zig-zag chains is of the order one (per nm) for an effective linker length of 20 bp as compared to the much larger value of $300\,nm^{-1}$ for naked DNA. Of course, depending on the values of α, β and linker length, this value varies over a wide range. Also the other mechanical parameters of the two-angle fiber indicate an extremely soft structure, as long as the elastic properties are determined by the DNA backbone alone. It is thus evident that the presence of the nucleosomes must play a crucial role in determining many of the mechanical properties of the 30-nm fiber. For instance, the excluded volume will not allow a strong fiber bending that would lead to overlapping nucleosomes, and the nucleosome-nucleosome attraction counteracts the stretching of the fiber under external tension.

To account for these effects, one has to go beyond the simple geometrical two-angle model and must include nucleosome-nucleosome interactions. On a purely theoretical level this is a hard task, and there have only been approximate estimates to the tension-induced condensation-decondensation transition of the fiber[17]. Numerical computer models are of great help to clarify the picture since it is relatively straightforward to build in linker elasticity, nucleosome/nucleosome

interactions and other force fields as they become necessary to describe structural details. Furthermore, while the two-angle model is of great help in exploring those regions of conformational space that are accessible to the chromatin chain, it generates very regular structures. Local variations in nucleosome positioning and, most importantly, thermal fluctuations at room temperature will cause random deviations from this regular structure; to understand the dynamics of the chromatin chain, it is very important to include these fluctuations into the model. The same issue has been discussed in the DNA field some time ago: while elastic rod models were successful in early theoretical descriptions of DNA supercoiling (e.g. [77; 78; 79], for review see[80]), the computation of real-life structural properties of superhelical DNA is only possible with numerical models that include thermal fluctuations (for a discussion of this point, see also[81]). Here we will therefore now consider methods that create configurational ensembles which reflect the structure of the chromatin chain at a finite temperature.

The chromatin chain at thermodynamic equilibrium

To find the equilibrium structure of the chromatin chain, one could try and minimize the total energy of the two-angle model computed numerically from appropriate elastic tension, electrostatic attraction/repulsion and other interaction potentials. This energy would then be minimized by standard minimization procedures, leading to a conformation at elastic equilibrium. If the molecule is small enough, its structural fluctuations will be small compared to its overall size, and then this simple energy minimization can in principle find a structure close to the structure free in solution at room temperature. However, in the case of a complex polymer chain typically only one or a few minimum energy conformations are predicted. As the temperature becomes larger than absolute zero (certainly at physiological temperatures), thermal motion leads to a multitude of possible conformations with almost the same energy; as long as the energy difference between two conformations is less than kT, both will be present at equilibrium with significant probability. The chance for the minimum elastic energy conformation to occur at thermodynamic equilibrium is actually very close to zero in this case.

Thus, to reflect correctly the state of the system at a certain temperature, one needs a simulation technique that generates an ensemble of chain conformations whose statistical properties reflect those of the 'real' chain at thermodynamic equilibrium. The chromatin fiber models that are discussed in the following all use one or another variation of such techniques.

Metropolis Monte-Carlo

Since minimum *energy* structures do not adequately describe the average structure of large biopolymers in an ensemble at thermodynamic equilibrium, one must minimize the *free energy*, which includes the configurational entropy of the structure. Depending on whether time dependent information is to be calculated, different approaches can be taken for such a minimization. A very popular method to sample the thermodynamic equilibrium of a system is known under the name of 'importance-sampling Monte-Carlo' and has been described half a century ago by Metropolis et al.[82]. The 'Metropolis Monte-Carlo' algorithm works as follows:

1. Starting from a given initial conformation with energy E_1, we generate a new "trial" conformation by a random variation (e.g. in the position or orientation of a subunit) and calculate its energy E_2. For a model chromatin chain, the total energy of each particular conformation can be very easily calculated if all the interaction energies between the constituents, DNA and nucleosomes, are known (as is the case for the interactions discussed above).
2. If $E_2 \leq E_1$, then we accept the new conformation into the ensemble.
3. If $E_2 > E_1$, we calculate the Boltzmann factor p for the increase in energy, $p = e^{-(E_2-E_1)/kT}$, and then compare this factor to a random number x between 0.0 and 1.0. If $p > x$, we accept the new conformation into the ensemble, otherwise we reject it and add the old conformation once more to the ensemble.

This algorithm will generate the ensemble of conformations at thermodynamic equilibrium, if the conformational variations introduced in step 1 (the so-called 'moves') are sufficient to cover all possible regions of conformational space and are locally reversible. It is easy to understand that feature of the Metropolis procedure: the transition probability into the higher energy state is

given by the Boltzmann factor, the transition probability into the lower energy state is one. The relative population of the two states is then the ratio of the transition probabilities, thus the Boltzmann factor; this is the outcome expected from thermodynamics.

Brownian dynamics simulation

For calculating the *time-dependent* properties of biopolymers, the equations of motion of the molecule in a viscous medium (i.e., water) under the influence of thermal motion must be solved. This can be done numerically by the method of Brownian dynamics (BD) [83]. Allison and coworkers [61; 62; 84] and later others [85; 86; 87; 88] have employed BD calculations to simulate the dynamics of linear and superhelical DNA; BD models for the chromatin chain will be discussed below.

Like in the case of Monte-Carlo, the internal energy of the chain is computed from the interaction potentials. Forces are then calculated from the derivatives of these energies with respect to the coordinates, and allowed to act during a certain time step (typically a few nanoseconds). This procedure will relax a given initial conformation into a state that fluctuates around the thermodynamic equilibrium. Since the motions at each step of the simulation come from the solution of equations of motion, including real forces, viscosities and thermal energies, the BD approach has the advantage that the calculated trajectories describe the real-time motion of the molecule in its solvent. Thus quantities related to the motions of the polymer like translational and rotational diffusion coefficients or internal relaxation modes can be obtained from the model using only the known physical properties of the constituents, as discussed above.

Monte Carlo modeling of the chromatin fiber

The first Monte-Carlo model of the chromatin chain was introduced by Katritch et al.[89] to interpret the stretching experiments on chromatin fibers by Cui and Bustamante[66]. Their model approximates the nucleosome as a spherical particle with an effective diameter between 11 and 20 nm and an optional attractive interaction. The linker DNA was modeled as a chain of rigid segments held together through bending and twisting potentials; the angle of the linker DNA at

the nucleosome was varied as one of the parameters used to fit the experimental data. Different from the two-angle model described above, the authors did not fix the value for the rotational angle Δ between each pair of neighboring nucleosomes. The energy function used in the Monte-Carlo model included a constant stretching force. The best fit to the experimental force-extension curves at low salt (5 mM) was obtained with an effective nucleosome diameter of 14 nm, a free linker length of 40 base pairs and a linker DNA opening angle of 50°. Other parameters of the model, such as the twist between nucleosomes, do not influence the computed force-extension characteristics significantly. To reproduce the response of chromatin fibers to extension at high salt conditions, it was necessary to introduce an attractive potential between closely spaced nucleosomes, which was a simple step function and radially symmetric. The equilibrium conformations of chromatin fibers generated by the model without an applied force, however, are quite irregular and do not resemble the typical 30 nm fiber; rather, even small (<2kT) internucleosomal attractions collapse the chain into a highly condensed form.

To overcome the restrictions of the Katritch model due to the approximation of the nucleosome as a sphere, Wedemann and Langowski[50] developed a Monte-Carlo model for the 30 nm fiber in which the nucleosome core particles are represented by oblate ellipsoids. The linker DNA was again described as a segmented elastic polymer, whose segments are connected by elastic bending, torsional, and stretching springs. The electrostatic interaction between the DNA segments was described by the Debye-Hückel approximation.

An important addition compared to previous models was the parameterization of the internucleosomal interaction potential in the form of an anisotropic attractive potential of the Lennard-Jones form, the so-called Gay-Berne potential[90]. Here, the depth and location of the potential minimum can be set independently for radial and axial interactions, effectively allowing the use of an ellipsoid as a good first-order approximation of the shape of the nucleosome. The potential had to be calibrated from independent experimental data, which exists, e.g., from the studies of mononucleosome liquid crystals by the Livolant group[44; 46] (see

above). The position of the potential minima in axial and radial direction were obtained from the periodicity of the liquid crystal in these directions, and the depth of the potential minimum was estimated from a simulation of liquid crystals using the same potential.

In order to connect the chromatin chain and to model the effect of the linker histone, DNA and chromatosomes were linked either at the surface of the chromatosome or through a rigid nucleosome stem 2 nm long. A Metropolis-Monte Carlo algorithm was then used to generate equilibrium ensembles of 100-nucleosome chains at physiological ionic strength. For a DNA linked at the nucleosome stem and a nucleosome repeat of 200 bp, the simulated fiber diameter of 32 nm and the mass density of 6.1 nucleosomes per 11 nm fiber length are in excellent agreement with the canonical value of 6 for the solenoid fiber as well as with experimental values from the literature, e.g. the neutron scattering data reported by Gerchman and Ramakrishnen[91] (other references given in [50]). The experimental value of the inclination of DNA and nucleosomes to the fiber axis[92] could also be reproduced.

One result of the simulations was that the torsion angle β between successive nucleosomes determines the properties of the structure to a great extent (as also predicted by the two-angle model). While a variation in the internucleosome interaction potential by a factor of four changes the simulated mass density by only about 5%, this quantity is very sensitive to variations in twist angle (see Fig. 6 in[50]).

The linker DNA connects chromatosomes on opposite sides of the fiber, and the overall packing of the nucleosomes leads to a helical aspect of the structure. The persistence length of simulated fibers with 200 bp repeat and stem is 265 nm. For more random fibers where the tilt angles between two nucleosomes are chosen according to a Gaussian distribution along the fiber, the persistence length decreases to 30 nm with increasing width of the distribution, while the other observable parameters such as the mass density remain unchanged. Polynucleosomes with repeat lengths of 212 bp also form fibers with the expected experimental properties. Systems with even

larger repeat length form fibers, but the mass density is significantly lower than the measured value. While a nucleosome chain without a stem (i.e., DNA and nucleosomes are connected at the core particle) and a repeat length of 192 bp gives stable fibers with linear mass densities in range with the experimental values, chains without a stem and a repeat length of 217 bp do not form fibers.

The persistence length computed from the bending fluctuations of the computed conformations shows an increase for shorter linker lengths, which confirms the tendency predicted by the simple two-angle model. However, the absolute values of the persistence length are between 60 and 260 nm, much higher than in the two-angle model, indicating that the nucleosome-nucleosome interactions are essential for controlling the mechanical properties of chromatin. Also, highly ordered chromatin structures are stiffer than more irregular ones: High values for the persistence length (200-300 nm) were obtained when the twist angle between adjacent nucleosomes was constant; when this twist was varied randomly, the persistence length decreased significantly.

Simulation of chromatin stretching

Cui and Bustamante[66], Bennink et al.[43], Brower-Toland et al.[42] and Leuba and Zlatanova (unpublished results) have reported single molecule stretching experiments on chromatin. For the force-extension curves, generally two regimes with different behavior can be distinguished: at low forces no structural transitions occur and the extension of the chain is determined solely by its elasticity, while at forces above 10-20 pN individual nucleosomes start to disintegrate. The dissociation of the NCPs that occurs at higher forces gives rise to distinct ‘jumps’ in the force-extension curve, whose amplitude is directly related to the length of DNA liberated during the dissociation[42; 43].The energetics of DNA unbinding from the histones have not been characterized in detail, although some estimates exist[93; 94]. Therefore, current computer models of the chromatin fiber do not yet include the ‘unrolling’ of the DNA from the nucleosome core

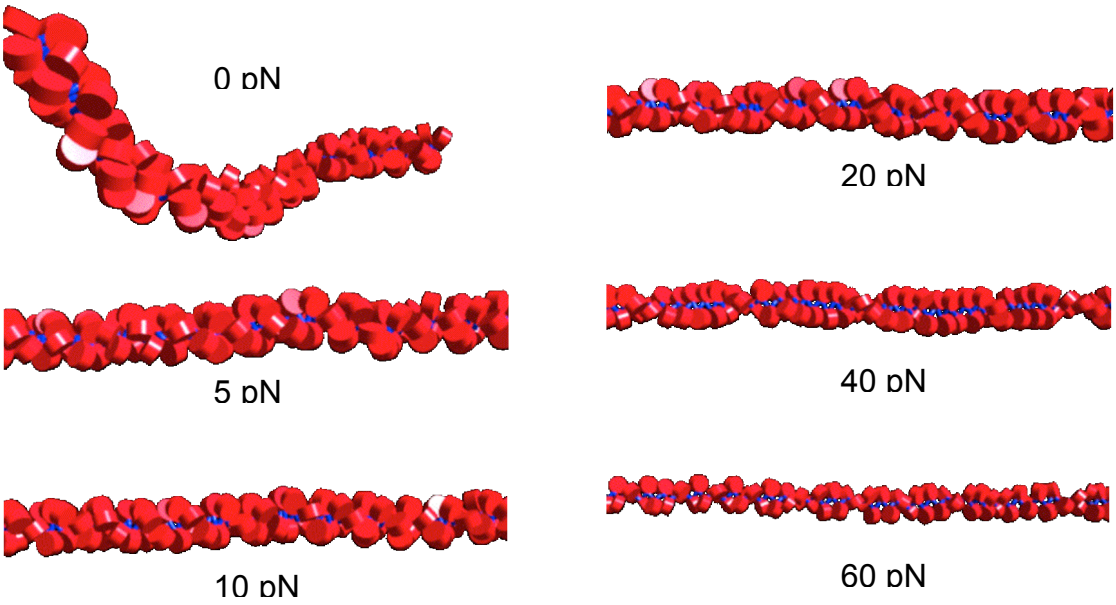

Fig. 5: Monte-Carlo simulation of the stretching of a chromatin chain. A 100 nucleosome chain with 200 bp repeat and 11 bp linker DNA was first equilibrated and then exposed to a pulling force as indicated below the drawings. For displaying the full chain, the scale of the picture was changed with increasing force. An unwinding of the chromatin fiber and sliding of the nucleosomes can be readily observed.

during stretching. We hope that this will become possible soon since a theoretical understanding of this process has now been achieved (I. Kulic and H. Schiessel, manuscript in preparation).

While structural transitions at the level of nucleosomes are still outside the scope of current models, applying a constant force to both ends of the fiber allows to simulate the low end of the force-extension curve. First results from our own work (Aumann, Caudron, Wedemann and Langowski, manuscript in preparation) are shown in Fig. 5. In this particular example, a nucleosome repeat of 200 bp and a linker DNA length of 11 bp was used.

The stretching modulus of the chromatin fiber can be extracted from the simulations in Fig. 5. Through a comparison with the third-power dependency predicted by the two-angle model[17] we can estimate that for linker lengths of 11-24 bp, stretching moduli of 50-5 pN are obtained, in line with the existing single molecule stretching data. A more detailed analysis of the dependence of the stretching rigidity on the local geometry of the chromatin fiber and on the internucleosomal interaction is under work.

Dynamic simulations of the chromatin fiber

For modeling time-dependent structural changes in the chromatin chain, time scales need to be used that are by far larger than the typical nanosecond range that is used in all-atom molecular dynamics. Conformational changes, internal motions, etc. of a large biomolecule occur on a millisecond time scale or longer. In order to reach this time scale in a simulation, the molecule has to be described by a coarse-grained model (see above), and the embedding solvent also needs to be approximated by a homogeneous fluid with given viscosity, dielectric constant and ion composition. The Brownian motion of the biomolecule, which is caused by the random thermal 'pushes' of the solvent molecules, is described by a random force.

In this type of modeling, called Brownian dynamics[83], an ensemble of conformations at thermodynamic equilibrium is generated in a way very analogous to the Monte-Carlo model: starting from an initial conformation, the model relaxes in steps towards the minimum free energy state. Other than in the Monte-Carlo method, however, the displacements of the subunits (beads and DNA segments) at each step are determined by the forces that act on each subunit, their viscous drag in the aqueous medium and the random force that corresponds to the thermal motion. In this way, real-time dynamics may be calculated for large systems, such as superhelical DNA[21; 95], chromatin chains[65; 96] or entire interphase chromosomes[97], over time scales of several hundred milliseconds.

Brownian dynamics models of the chromatin fiber

In an early attempt to model the dynamics of the chromatin fiber, Ehrlich and Langowski[96] assumed a chain geometry similar to the one used later by Katritch et al.[89]: nucleosomes were approximated as spherical beads and the linker DNA as a segmented flexible polymer with Debye-Hückel electrostatics. The interaction between nucleosomes was a steep repulsive Lennard-Jones type potential; attractive interactions were not included.

With this model, dynamics of dinucleosomes could be simulated for trajectories of 50 μs within a couple of hours of CPU time. From these trajectories, diffusion coefficients were extracted

and compared with the light scattering data of Yao et al.[98]. The salt-dependent increase of the diffusion coefficient could be reproduced quantitatively, using a linker length of 76 bp, an effective hydrodynamic radius of the nucleosome of 5.95 nm and a linker DNA bending angle of 40°. Also, the simulated sedimentation coefficients showed good agreement with the experiments of Butler and Thomas[99]. The ionic strength dependence of the diffusion coefficient was interpreted by a change in the conformation of the linker DNA opening angle rather than changed bending of the linker DNA.

The missing internucleosome attraction, however, led to problems when longer nucleosome chains were simulated. Starting from an extended zig-zag conformation, folding of a 25-nucleosome chain occurred within 200 μs and the diameter of the resulting fiber-like structure was 45 nm in approximate agreement with values measured for chicken erythrocyte chromatin. On the other hand, the structure showed no regular helical arrangement of the nucleosomes, and the mass density of 1.3 nucleosomes/11 nm was much less than typical experimental values.

A more detailed view of the dynamics of a chromatin chain was achieved in a recent Brownian dynamics simulation by Beard and Schlick[65]. Like in previous work, the DNA is treated as a segmented elastic chain; however, the nucleosomes are modeled as flat cylinders with the DNA attached to the cylinder surface at the positions known from the crystallographic structure of the nucleosome. Moreover, the electrostatic interactions are treated in a very detailed manner: the charge distribution on the nucleosome core particle is obtained from a solution to the nonlinear Poisson-Boltzmann equation in the surrounding solvent, and the total electrostatic energy is computed through the Debye-Hückel approximation over all charges on the nucleosome and the linker DNA.

Using this model, the authors performed Brownian dynamics simulations with a time step of 2 ps and maximum simulation times of 50 ns for a 48-nucleosome chain and 100 ns for di- and trinucleosomes. Like in the previous work of Ehrlich et al.[96] the oligonucleosome trajectories

were used to compute diffusion coefficients and compare them to the experimental data by Yao et al.[98] and Bednar et al.[16]. The study does predict a salt-dependent compaction of the oligonucleosomes, which manifests itself in an increased diffusion coefficient; within the limits of salt concentration studied, the authors obtained good quantitative agreement with the experimental data. The simulations on the 48-nucleosome chain show a stable 30 nm diameter zig-zag fiber at 50 mM salt, which unfolds when the salt concentration is decreased to 10 mM. Due to the computational requirements of the dynamics simulation, only the initial phase of the unfolding could be simulated and the equilibrium configuration was obtained through a Monte-Carlo simulation using the same energetics as the BD model.

The flexibility of the 30 nm fiber

For understanding the folding of the chromatin chain into interphase and metaphase chromosomes, an important quantity to be known is its flexibility, expressed as the bending persistence length. Distance distribution analysis for genetic marker pairs in human fibroblast nuclei [100; 101; 102] suggested a wormlike chain conformation for the 30 nm fiber with a persistence length L_p=100-140 nm. On the other hand, scanning force microscopy analysis of end-to-end distances of chromatin fibers on a mica surface gave L_p = 30-50 nm (Castro[103] as cited by Houchmanzadeh[104]), but the binding conditions of the fiber to the mica will influence the measured persistence length to a great extent (Bussiek, Mücke and Langowski, submitted to J. Mol. Biol.). At low salt concentrations, stretching experiments of single chromatin fibers from chicken erythrocytes with laser tweezers yielded L_p = 30 nm[66], but no data for the persistence length at physiological salt was given there. Two in vivo studies have been published, where recombination frequencies in human cells[105] or formaldehyde crosslinking probabilities in yeast[106] have been used to measure relative end-to-end distances. These studies report rather small persistence lengths of 30-50 nm. Thus, the experimental values for L_p in the literature span a rather large range of 30-140 nm, where the smaller values were obtained either on chromatin fibers in low salt or on chromosomes that were constrained in the volume of a

nucleus. Our recent simulations of the 30 nm chromatin fiber structure reported above suggest a rather stiff chain of $L_p \approx 250$ nm for very regular nucleosome spacing and short linkers, which decreases for more irregularly spaced nucleosomes or longer linkers.

The small persistence length obtained in vivo by recombination or crosslinking experiments, however, may correspond to a chromatin fiber stiffness several times higher than that estimated from the measured L_p alone. The persistence length is computed from distance measurements assuming an unconstrained self-crossing random walk. Since this condition is only fulfilled for the interphase chromatin fiber over rather short distances, the measured apparent L_p will depend, for a given chain flexibility, on the folding topology and the region or genomic separation for which it is calculated. The apparent L_p decreases with increasing compaction of the chromatin fiber relative to a random walk, because the assumption of a free wormlike chain breaks down. In recent model calculations of the arrangement of a 30 nm fiber with a *free* persistence length of $L_p = 150$ nm in interphase chromosomes (T. A. Knoch, Ph.D. thesis, University of Heidelberg, Knoch and Langowski, manuscript in preparation) we find that the folding topology may reduce the *apparent* persistence length quite dramatically.

This shows that the chromatin chain flexibility can only be reliably obtained from genomic distance measurements when an unconstrained random walk behavior of the chromatin fiber is assured[100; 101]. On the other hand this might explain the rather big differences in experimental values for the chromatin persistence length[100; 101; 102; 107; 108]. The in vivo studies that determined the persistence length indirectly by recombination[105] or crosslinking techniques[106] probably overestimate the chromatin fiber flexibility, because the external constraints such as folding topology and finite nuclear volume have not been taken into account. At any rate, a persistence length for the unconstrained chromatin fiber that is comparable to its diameter would give rise to structures that are so irregular that the notion of a 'fiber' breaks down completely. Comparison with numerical simulations, however, might allow extraction of physical properties of the chromatin fiber from sufficiently detailed experimental data.

Conclusion

Let us summarize the state of our understanding of the physics of chromatin folding by saying that the current knowledge about the structure and interaction of the basic components of chromatin – histones and DNA – enables us to develop the first quantitative models of the structure and dynamics of the chromatin fiber. Even so, these models are still at a very rudimentary stage: data on the interaction of the histone tails with their surroundings, on DNA binding/unbinding at the nucleosome surface, nucleosome/nucleosome interactions, the role of histone modifications and other chromatin-associated proteins are badly needed. However, biophysical techniques together with computational modeling and the ever-expanding body of such quantitative data hold a promising outlook for a much more detailed picture of the chromatin fiber in the years to come.

References

1. Zentgraf, H. & Franke, W. W. (1984). Differences of supranucleosomal organization in different kinds of chromatin: cell type-specific globular subunits containing different numbers of nucleosomes. *J Cell Biol* 99, 272-86.
2. Olins, A. L. & Olins, D. E. (1973). Spheroid chromatin units (v bodies). *Journal of Cell Biology* 59, 252a.
3. Olins, A. L. & Olins, D. E. (1974). Spheroid chromatin units (v bodies). *Science* 183, 330-2.
4. Woodcock, C. L. F. (1973). Ultrastructure of inactive chromatin. *Journal of Cell Biology* 59, 368a.
5. van Holde, K. & Zlatanova, J. (1995). Chromatin higher order structure: Chasing a mirage? *The Journal of Biological Chemistry* 270, 8373-8376.
6. van Holde, K. & Zlatanova, J. (1996). What determines the folding of the chromatin fiber. *Proceedings of the National Academy of Sciences of the USA* 93, 10548-10555.
7. van Holde, K. E. (1989). *Chromatin*, Springer, Heidelberg.
8. Widom, J. (1989). Toward a unified model of chromatin folding. *Annu Rev Biophys Biophys Chem* 18, 365-95.
9. Finch, J. T. & Klug, A. (1976). Solenoidal model for superstructure in chromatin. *Proceedings of the National Academy of Sciences of the USA* 73, 1897-1901.
10. Thoma, F., Koller, T. & Klug, A. (1979). Involvement of histone H1 in the organization of the nucleosome and of the salt-dependent superstructures of chromatin. *J Cell Biol* 83, 403-27.
11. Widom, J. & Klug, A. (1985). Structure of the 300A chromatin filament: X-ray diffraction from oriented samples. *Cell* 43, 207-13.
12. Woodcock, C. L., Grigoryev, S. A., Horowitz, R. A. & Whitaker, N. (1993). A chromatin folding model that incorporates linker variability generates fibers resembling the native structures. *Proceedings of the National Academy of Sciences of the USA* 90, 9021-9025.
13. Horowitz, R. A., Agard, D. A., Sedat, J. W. & Woodcock, C. L. (1994). The three-dimensional architecture of chromatin in situ: electron tomography reveals fibers composed of a continuously variable zig-zag nucleosomal ribbon. *J Cell Biol* 125, 1-10.
14. Woodcock, C. L. & Dimitrov, S. (2001). Higher-order structure of chromatin and chromosomes. *Curr Opin Genet Dev* 11, 130-5.
15. Leuba, S. H., Yang, G., Robert, C., Samori, B., van Holde, K., Zlatanova, J. & Bustamante, C. (1994). Three-dimensional structure of extended chromatin fibers as revealed by tapping-mode scanning force microscopy. *Proceedings of the National Academy of Sciences of the USA* 91, 11621-11625.
16. Bednar, J., Horowitz, R. A., Grigoryev, S. A., Carruthers, L. M., Hansen, J. C., Koster, A. J. & Woodcock, C. L. (1998). Nucleosomes, linker DNA, and linker histone form a unique structural motif that directs the higher-order folding and compaction of chromatin. *Proceedings of the National Academy of Sciences of the USA* 95, 14173-14178.
17. Schiessel, H., Gelbart, W. M. & Bruinsma, R. (2001). DNA folding: Structural and mechanical properties of the two- angle model for chromatin. *Biophysical Journal* 80, 1940-1956.
18. Stigter, D. (1977). Interactions of highly charged colloidal cylinders with applications to double stranded DNA. *Biopolymers* 16, 1435-1448.
19. Klenin, K. V., Frank-Kamenetskii, M. D. & Langowski, J. (1995). Modulation of intramolecular interactions in superhelical DNA by curved sequences: a Monte Carlo simulation study. *Biophysical Journal* 68, 81-88.
20. Delrow, J. J., Gebe, J. A. & Schurr, J. M. (1997). Comparison of hard-cylinder and screened Coulomb interactions in the modeling of supercoiled DNAs. *Biopolymers* 42, 455-70.

21. Klenin, K., Merlitz, H. & Langowski, J. (1998). A Brownian dynamics program for the simulation of linear and circular DNA and other wormlike chain polyelectrolytes. *Biophys J* 74, 780-788.
22. Merlitz, H., Rippe, K., Klenin, K. V. & Langowski, J. (1998). Looping dynamics of linear DNA molecules and the effect of DNA curvature: a study by Brownian dynamics simulation. *Biophysical Journal* 74, 773-779.
23. Rybenkov, V. V., Cozzarelli, N. R. & Vologodskii, A. V. (1993). Probability of DNA knotting and the effective diameter of the DNA double helix. *Proceedings of the National Academy of Sciences of the USA* 90, 5307-5311.
24. Rybenkov, V. V., Vologodskii, A. V. & Cozzarelli, N. R. (1997). The effect of ionic conditions on DNA helical repeat, effective diameter and free energy of supercoiling. *Nucleic Acids Res* 25, 1412-1418.
25. Hammermann, M., Steinmaier, C., Merlitz, H., Kapp, U., Waldeck, W., Chirico, G. & Langowski, J. (1997). Salt effects on the structure and internal dynamics of superhelical DNAs studied by light scattering and Brownian dynamics. *Biophys J* 73, 2674-87.
26. Hammermann, M., Brun, N., Klenin, K. V., May, R., Toth, K. & Langowski, J. (1998). Salt-dependent DNA superhelix diameter studied by small angle neutron scattering measurements and Monte Carlo simulations. *Biophys J* 75, 3057-3063.
27. Lu, Y., Weers, B. & Stellwagen, N. C. (2001). DNA persistence length revisited. *Biopolymers* 61, 261-75.
28. Barkley, M. D. & Zimm, B. H. (1979). Theory of twisting and bending of chain macromolecules: analysis of the fluorescence depolarization of DNA. *Journal of Chemical Physics* 70, 2991-3007.
29. Fujimoto, B. S. & Schurr, J. M. (1990). Dependence of the torsional rigidity of DNA on base composition. *Nature* 344, 175-7.
30. Schurr, J. M., Fujimoto, B. S., Wu, P. & Song, L. (1992). Fluorescence studies of nucleic acids: dynamics, rigidities and structures. In *Topics in Fluorescence Spectroscopy* (Lakowicz, J. R., ed.), Vol. 3, pp. 137-229. Plenum Press, New York.
31. Shore, D. & Baldwin, R. L. (1983). Energetics of DNA twisting. I. Relation between twist and cyclization probability. *Journal of Molecular Biology* 179, 957-981.
32. Horowitz, D. S. & Wang, J. C. (1984). Torsonal Rigidity of DNA and Length Dependence of the Free Energy of DNA Supercoiling. *J. Mol. Biol.* 173, 75-91.
33. Taylor, W. H. & Hagerman, P. J. (1990). Application of the method of phage T4 DNA ligase-catalyzed ring-closure to the study of DNA structure I.NaCl-dependence of DNA flexibility and helical repeat. *J. Mol. Biol.* 212, 363-376.
34. Cluzel, P., Lebrun, A., Heller, C., Lavery, R., Viovy, J.-L., Chatenay, D. & Caron, F. (1996). DNA: An extensible molecule. *Science* 271, 792-794.
35. Smith, S. B., Cui, Y. & Bustamante, C. (1996). Overstretching B-DNA: the elastic response of individual double-stranded and single-stranded DNA molecules. *Science* 271, 795-799.
36. Lankas, F., Sponer, J., Hobza, P. & Langowski, J. (2000). Sequence-dependent Elastic Properties of DNA. *J Mol Biol* 299, 695-709.
37. Lankas, F., Cheatham, I. T., Spackova, N., Hobza, P., Langowski, J. & Sponer, J. (2002). Critical effect of the N2 amino group on structure, dynamics, and elasticity of DNA polypurine tracts. *Biophys J* 82, 2592-609.
38. Arents, G., Burlingame, R. W., Wang, B.-C., Love, W. E. & Moudrianakis, E. N. (1991). The nucleosomal core histone octamer at 3.1 Å resolution: A triparatite protein assembly and a left-handed superhelix. *Proceedings of the National Academy of Sciences of the USA* 88, 10148-10152.
39. Luger, K., Mäder, A. W., Richmond, R. K., Sargent, D. F. & Richmond, T. J. (1997). Crystal structure of the nucleosome core particle at 2.8 Å resolution. *Nature* 389, 251-260.
40. Sivolob, A., DeLucia, F., Révet, B. & Prunell, A. (1999). Nucleosome dynamics. II. High flexibility of nucleosome entering and exiting DNAs to positive crossing. An ethidium

bromide fluorescence study of mononucleosomes on DNA minicircles. *J Mol Biol* 285, 1081-1099.
41. Sivolob, A. & Prunell, A. (2000). Nucleosome dynamics V. Ethidium bromide versus histone tails in modulating ethidium bromide-driven tetrasome chiral transition. A fluorescence study of tetrasomes on DNA minicircles. *J Mol Biol* 295, 41-53.
42. Brower-Toland, B. D., Smith, C. L., Yeh, R. C., Lis, J. T., Peterson, C. L. & Wang, M. D. (2002). Mechanical disruption of individual nucleosomes reveals a reversible multistage release of DNA. *Proc Natl Acad Sci U S A* 99, 1960-5.
43. Bennink, M. L., Leuba, S. H., Leno, G. H., Zlatanova, J., de Grooth, B. G. & Greve, J. (2001). Unfolding individual nucleosomes by stretching single chromatin fibers with optical tweezers. *Nat Struct Biol* 8, 606-10.
44. Leforestier, A. & Livolant, F. (1997). Liquid crystalline ordering of nucleosome core particles under macromolecular crowding conditions: evidence for a discotic columnar hexagonal phase. *Biophys J* 73, 1771-6.
45. Livolant, F. & Leforestier, A. (2000). Chiral discotic columnar germs of nucleosome core particles. *Biophys J* 78, 2716-29.
46. Leforestier, A., Dubochet, J. & Livolant, F. (2001). Bilayers of nucleosome core particles. *Biophys J* 81, 2414-21.
47. Mangenot, S., Leforestier, A., Durand, D. & Livolant, F. (2003). X-ray diffraction characterization of the dense phases formed by nucleosome core particles. *Biophys J* 84, 2570-84.
48. Mangenot, S., Leforestier, A., Vachette, P., Durand, D. & Livolant, F. (2002). Salt-induced conformation and interaction changes of nucleosome core particles. *Biophys J* 82, 345-56.
49. Mangenot, S., Raspaud, E., Tribet, C., Belloni, L. & Livolant, F. (2002). Interactions between isolated nucleosome core particles: A tail-bridging effect? *European Physical Journal E* 7, 221-231.
50. Wedemann, G. & Langowski, J. (2002). Computer simulation of the 30-nanometer chromatin fiber. *Biophys J* 82, 2847-59.
51. Beard, D. A. & Schlick, T. (2001). Modeling salt-mediated electrostatics of macromolecules: the discrete surface charge optimization algorithm and its application to the nucleosome. *Biopolymers* 58, 106-15.
52. Matsumoto, A. & Go, N. (1999). Dynamic properties of double-stranded DNA by normal mode analysis. *J Chem Phys* 110, 11070-11075.
53. Matsumoto, A. & Olson, W. K. (2002). Sequence-dependent motions of DNA: a normal mode analysis at the base-pair level. *Biophys J* 83, 22-41.
54. Cheatham, T. E., 3rd & Young, M. A. (2000). Molecular dynamics simulation of nucleic acids: successes, limitations, and promise. *Biopolymers* 56, 232-56.
55. Klenin, K. V., Vologodskii, A. V., Anshelevich, V. V., Dykhne, A. M. & Frank-Kamenetskii, M. D. (1988). Effect of excluded volume on topological properties of circular DNA. *Journal of Biomolecular Structure & Dynamics* 5, 1173-1185.
56. Vologodskii, A. V., Levene, S. D., Klenin, K. V., Frank-Kamenetskii, M. & Cozzarelli, N. R. (1992). Conformational and thermodynamic properties of supercoiled DNA. *J Mol Biol* 227, 1224-43.
57. Langowski, J., Kapp, U., Klenin, K. & Vologodskii, A. (1994). Solution structure and dynamics of DNA topoisomers. Dynamic light scattering studies and Monte-Carlo simulations. *Biopolymers* 34, 639-646.
58. Rybenkov, V. V., Vologodskii, A. V. & Cozzarelli, N. R. (1997). The effect of ionic conditions on the conformations of supercoiled DNA .1. Sedimentation analysis. *J Mol Biol* 267, 299-311.
59. Huang, J., Schlick, T. & Vologodskii, A. (2001). Dynamics of site juxtaposition in supercoiled DNA. *Proc Natl Acad Sci U S A* 98, 968-73.

60. Fujimoto, B. S. & Schurr, J. M. (2002). Monte Carlo simulations of supercoiled DNAs confined to a plane. *Biophys J* 82, 944-62.
61. Allison, S. A. & McCammon, J. A. (1984). Transport Properties of Rigid and Flexible Macromolecules by Brownian Dynamics Simulation. *Biopolymers* 23, 167-187.
62. Allison, S. A. (1986). Brownian dynamics simulation of wormlike chains. Fluorescence depolarization and depolarized light scattering. *Macromolecules* 19, 118-124.
63. Allison, S. A., Sorlie, S. S. & Pecora, R. (1990). Brownian dynamics simulations of wormlike chains: Dynamic light scattering from a 2311 base pair DNA fragment. *Macromolecules* 23, 1110-1118.
64. Gebe, J. A., Allison, S. A., Clendenning, J. B. & Schurr, J. M. (1995). Monte-Carlo Simulations of Supercoiling Free-Energies for Unknotted and Trefoil Knotted DNAs. *Biophysical Journal* 68, 619-633.
65. Beard, D. A. & Schlick, T. (2001). Computational Modeling Predicts the Structure and Dynamics of Chromatin Fiber. *Structure* 9, 105-114.
66. Cui, Y. & Bustamante, C. (2000). Pulling a single chromatin fiber reveals the forces that maintain its higher-order structure. *Proceedings of the National Academy of Sciences of the USA* 97, 127-132.
67. Schiessel, H., Widom, J., Bruinsma, R. F. & Gelbart, W. M. (2001). Polymer Reptation and Nucleosome Repositioning. *Phys Rev Lett* 86, 4414-4417.
68. Bishop, T. C. & Hearst, J. E. (1998). Potential function describing the folding of the 30 nm fiber. *Journal of Physical Chemistry B* 102, 6433-6439.
69. Bishop, T. C. & Zhmudsky, O. O. (2002). Mechanical model of the nucleosome and chromatin. *Journal of Biomolecular Structure & Dynamics* 19, 877-887.
70. Zlatanova, J., Leuba, S. H. & van Holde, K. (1998). Chromatin fiber structure: morphology, molecular determinants, structural transitions. *Biophys J* 74, 2554-66.
71. Widom, J. (1992). A relationship between the helical twist of DNA and the ordered positioning of nucleosomes in all eukaryotic cells. *Proc Natl Acad Sci U S A* 89, 1095-9.
72. Schiessel, H. (2003). The physics of chromatin. *Journal of Physics: Condensed Matter* in press.
73. Daban, J. R. (2000). Physical constraints in the condensation of eukaryotic chromosomes. Local concentration of DNA versus linear packing ratio in higher order chromatin structures. *Biochemistry* 39, 3861-3866.
74. vanHolde, K. & Zlatanova, J. (1996). What determines the folding of the chromatin fiber? *Proceedings of the National Academy of Sciences of the United States of America* 93, 10548-10555.
75. Schiessel, H. (2002). How short-ranged electrostatics controls the chromatin structure on much larger scales. *Europhysics Letters* 58, 140-146.
76. Ben-Haim, E., Lesne, A. & Victor, J. M. (2001). Chromatin: a tunable spring at work inside chromosomes. *Phys Rev E Stat Nonlin Soft Matter Phys* 64, 051921.
77. Fuller, F. B. (1971). The writhing number of a space curve. *Proceedings of the National Academy of Sciences of the USA* 68, 815-819.
78. Benham, C. J. (1978). The statistics of superhelicity. *J Mol Biol* 123, 361-70.
79. Benham, C. J. (1977). Elastic model of supercoiling. *Proc Natl Acad Sci U S A* 74, 2397-401.
80. Olson, W. K. & Zhurkin, V. B. (2000). Modeling DNA deformations. *Curr Opin Struct Biol* 10, 286-97.
81. Langowski, J., Olson, W. K., Pedersen, S. C., Tobias, I., Westcott, T. P. & Yang, Y. (1996). DNA supercoiling, localized bending and thermal fluctuations. *Trends Biochem Sci* 21, 50.
82. Metropolis, N., Rosenbluth, A. W., Rosenbluth, M. N., Teller, A. H. & Teller, E. (1953). Equation of state calculations by fast computing machines. *The Journal of Chemical Physics* 21, 1087-1092.

83. Ermak, D. L. & McCammon, J. A. (1978). Brownian dynamics with hydrodynamic interactions. *Journal of Chemical Physics* 69, 1352-1359.
84. Allison, S. A., Austin, R. & Hogan, M. (1989). Bending and Twisting Dynamics of Short Linear DNAs - Analysis of the Triplet Anisotropy Decay of a 209-Base Pair Fragment by Brownian Simulation. *Journal of Chemical Physics* 90, 3843-3854.
85. Chirico, G. & Langowski, J. (1992). Calculating hydrodynamic properties of DNA through a second-order Brownian dynamics algorithm. *Macromolecules* 25, 769-775.
86. Chirico, G. & Langowski, J. (1994). Kinetics of DNA supercoiling studied by Brownian dynamics simulation. *Biopolymers* 34, 415-433.
87. Chirico, G. & Langowski, J. (1996). Brownian dynamics simulations of supercoiled DNA with bent sequences. *Biophys J* 71, 955-71.
88. Garcia de la Torre, J., Navarro, S. & Lopez Martinez, M. C. (1994). Hydrodynamic Properties of a Double-Helical Model for DNA. *Biophysical Journal* 66, 1573-1579.
89. Katritch, V., Bustamante, C. & Olson, V. K. (2000). Pulling chromatin fibers: Computer simulations of direct physical micromanipulations. *Journal of Molecular Biology* 295, 29-40.
90. Gay, J. G. & Berne, B. J. (1981). Modification of the overlap potential to mimic a linear site--site potential. *Journal of Chemical Physics* 74, 3316--3319.
91. Gerchman, S. E. & Ramakrishnan, V. (1987). Chromatin higher-order structure studied by neutron scattering and scanning transmission electron microscopy. *Proceedings of the National Academy of Sciences of the USA* 84, 7802-7806.
92. Dimitrov, S. I., Makarov, V. L. & Pashev, I. G. (1990). The chromatin fiber: structure and conformational transitions as revealed by optical anisotropy studies. *J Biomol Struct Dyn* 8, 23-35.
93. Widlund, H. R., Vitolo, J. M., Thiriet, C. & Hayes, J. J. (2000). DNA sequence-dependent contributions of core histone tails to nucleosome stability: Differential effects of acetylation and proteolytic tail removal. *Biochemistry* 39, 3835-3841.
94. Thastrom, A., Lowary, P. T., Widlund, H. R., Cao, H., Kubista, M. & Widom, J. (1999). Sequence motifs and free energies of selected natural and non-natural nucleosome positioning DNA sequences. *J Mol Biol* 288, 213-29.
95. Wedemann, G., Münkel, C., Schoppe, G. & Langowski, J. (1998). Kinetics of structural changes in superhelical DNA. *Physical Review E* 58, 3537-3546.
96. Ehrlich, L., Munkel, C., Chirico, G. & Langowski, J. (1997). A Brownian dynamics model for the chromatin fiber. *Comput Appl Biosci* 13, 271-9.
97. Münkel, C. & Langowski, J. (1998). Chromosome structure described by a polymer model. *Physical Review E* 57, 5888-5896.
98. Yao, J., Lowary, P. T. & Widom, J. (1990). Direct detection of linker DNA bending in defined-length oligomers of chromatin. *Proceedings of the National Academy of Sciences of the USA* 87, 7603-7607.
99. Butler, P. J. & Thomas, J. O. (1998). Dinucleosomes show compaction by ionic strength, consistent with bending of linker DNA. *Journal of Molecular Biology* 281, 401-407.
100. van den Engh, G., Sachs, R. & Trask, B. J. (1992). Estimating genomic distance from DNA sequence location in cell nuclei by a random walk model. *Science* 257, 1410-1412.
101. Trask, B. J., Allen, S., Massa, H., Fertitta, A., Sachs, R., van den Engh, G. & Wu, M. (1993). Studies of metaphase and interphase chromosomes using fluorescence in situ hybridization. *Cold Spring Harb Symp Quant Biol* 58, 767-75.
102. Yokota, H., van den Engh, G., Hearst, J., Sachs, R. K. & Trask, B. J. (1995). Evidence for the organization of chromatin in megabase pair-sized loops arranged along a random walk path in the human G0/G1 interphase nucleus. *The Journal of Cell Biology* 130, 1239-1249.
103. Castro, C. (1994). Measurement of the elasticity of single chromatin fibers: the effect of histone H1. PhD Thesis, University of Oregon, Eugene.

104. Houchmandzadeh, B., Marko, J. F., Chatenay, D. & Libchaber, A. (1997). Elasticity and structure of eukaryote chromosomes studied by micromanipulation and micropipette aspiration. *J. Cell. Biol.* 139, 1-12.
105. Ringrose, L., Chabanis, S., Angrand, P. O., Woodroofe, C. & Stewart, A. F. (1999). Quantitative comparison of DNA looping *in vitro* and *in vivo*: chromatin increases effective DNA flexibility at short distances. *The EMBO Journal* 18, 6630-6641.
106. Dekker, J., Rippe, K., Dekker, M. & Kleckner, N. (2002). Capturing Chromosome Conformation. *Science* 295, 1306-1311.
107. Ostashevsky, J. Y. & Lange, C. S. (1994). The 30 nm chromatin fiber as a flexible polymer. *Journal of Biomolecular Structure & Dynamics* 11, 813-820.
108. Sachs, R. K., van den Engh, G., Trask, B., Yokota, H. & Hearst, J. E. (1995). A random-walk/giant-loop model for interphase chromosomes. *Proceedings of the National Academy of Sciences of the USA* 92, 2710-2714.